

1 **High-Resolution Melt Curve Analysis: An Approach for Mutation** 2 **Detection in the TPO Gene of Congenital Hypothyroid Patients in** 3 **Bangladesh**

4
5 Mst. Noorjahan Begum^{1,2,3}, Rumana Mahtarin², Md Tarikul Islam², Nusrat Jahan Antora²,
6 Suprovath Kumar Sarker², Nusrat Sultana², Abu A. Sajib¹, Abul B.M.M.K Islam¹, Hurjahan
7 Banu⁴, M A Hasanat⁴, Kohinoor Jahan Shyamaly⁵, Suraiya Begum⁵, Tasnia Kawsar Konika⁶,
8 Shahinur Haque⁶, Mizanul Hasan⁶, Sadia Sultana⁷, Taufiqur Rahman Bhuiyan⁸, Kaiissar
9 Mannoor², Firdausi Qadri^{2,8}, Sharif Akhteruzzaman^{1*}

10
11 ¹Department of Genetic Engineering & Biotechnology, University of Dhaka, Dhaka-1000,
12 Bangladesh.

13 ²Institute for Developing Science and Health Initiatives (ideSHi), ECB Chattar, Mirpur, Dhaka,
14 Bangladesh.

15 ³Virology Laboratory, Infectious Diseases Division, International Centre for Diarrhoeal Disease
16 Research, Bangladesh, Mohakhali, Dhaka-1212, Bangladesh.

17 ⁴Department of Endocrinology, Bangabandhu Sheikh Mujib Medical University (BSMMU),
18 Shahbag, Dhaka-1000, Bangladesh.

19 ⁵Department of Pediatrics, Bangabandhu Sheikh Mujib Medical University (BSMMU) Shahbag,
20 Dhaka-1000, Bangladesh.

21 ⁶Nuclear Medicine and Allied Sciences, Bangabandhu Sheikh Mujib Medical University
22 (BSMMU), Shahbag, Dhaka-1000, Bangladesh.

23 ⁷Scintigraphy Division, Bangabandhu Sheikh Mujib Medical University (BSMMU) Shahbag,
24 Dhaka-1000, Bangladesh.

25 ⁸Mucosal Immunology and Vaccinology, Infectious Diseases Division, International Centre for
26 Diarrhoeal Disease Research, Bangladesh, Mohakhali, Dhaka-1212, Bangladesh.

27
28 *Correspondence: sazaman@du.ac.bd

30 **Abstract**

31 Thyroid Peroxidase (*TPO*) is known to be the major gene involved in Congenital hypothyroid
32 patients with thyroid dyshormonogenesis. This present study aimed to establish high-resolution
33 melting (HRM) curve analysis as a supplementary mutation detection approach of Sanger
34 sequencing targeting commonly found mutations c.1117G>T, c.1193G>C, and c.2173A>C in the
35 *TPO* gene in Bangladeshi patients. We enrolled 36 confirmed cases of congenital hypothyroid
36 patients with dyshormonogenesis to establish the HRM method. Blood samples were collected,
37 and genomic DNA was isolated for molecular techniques. Among the 36 specimens, 20 were pre-
38 sequenced, and mutations were characterized through Sanger sequencing. The pre-sequenced
39 specimens (n=20) were then subjected to real-time PCR-HRM curve analysis to get the appropriate
40 HRM condition capable of differentiating heterozygous and homozygous states for the three
41 mutations from the wild-type state. Furthermore, 16 unknown specimens were subjected to HRM
42 analysis to validate the method. This method showed 100 percent sensitivity and specificity to
43 distinguish wild-type alleles from homozygous or heterozygous states (c.1117G>T, c.1193G>C,
44 and c.2173A>C) of alleles commonly found in Bangladeshi patients. The HRM data was found to
45 be similar to the sequencing result, thus confirming the validity of the HRM approach for *TPO*
46 gene mutation.

47 In conclusion, the established HRM-based molecular technique targeting c.1117G>T, c.1193G>C,
48 and c.2173A>C mutations could be used as a high throughput, rapid, reliable, and cost-effective
49 screening approach for the detection of all common mutations in *TPO* gene in Bangladeshi patients
50 with dyshormonogenesis.

51

52 **Key words:** Congenital Hypothyroidism, Thyroid Dyshormonogenesis, Thyroid Peroxidase,
53 High-Resolution Melt Curve Analysis

54

55 1. Introduction

56 Congenital hypothyroidism (CH) is the endocrine disorder in which thyroid hormone deficiency
57 occurs at birth and is the most common preventable cause of mental retardation [1-3]. This
58 condition can lead to different clinical complications such as irreversible brain damage, delayed
59 developmental milestones, lethargy, and slowdown of the body's overall metabolism of the
60 patients if untreated. Early detection and initiation of treatment can reverse such complications [4].
61 The CH frequency is 1 in 3000-4000 newborns worldwide, whereas it is much higher in
62 Bangladesh [5-9]. 11 genes, including thyroid gland development and thyroid hormone
63 biosynthesis, have been documented [10]. A defect in thyroid gland development due to mutations
64 in both gene alleles of the pathway is known as thyroid dysgenesis. In contrast, a defect in thyroid
65 hormone biosynthesis due to mutations in both alleles of a gene of the pathway is called thyroid
66 dyshormonogenesis (TDH). TDH occurs due to mutations commonly found in seven genes,
67 including TPO as a significant contributor to them [11, 12]. Since thyroid hormones are iodinated,
68 TPO catalyzes the iodination steps, and mutations in the TPO gene may cause either total iodide
69 organification defect (TIOD) or partial iodine organification defect (PIOD). Different countries
70 conducted several studies on screening and identification of mutations in the TPO gene causing
71 TIOD and PIOD [13-18]. Our previous study investigated that only genetic causes accounted for
72 all of the CH patients with dyshormonogenesis in hospital settings in Bangladesh and didn't find
73 any other aetiology [19]. Since CH is easily treatable, it is important to investigate the aetiology,
74 which would help to determine how long the patients need hormone replacement therapy. The CH
75 patients with genetic aetiology need lifelong hormone therapy [20]. Sometimes, neonatal CH
76 screening using biochemical tests becomes difficult due to the presence of maternal TSH in the
77 specimens of neonates, and this problem can be overcome by genetic screening at an early age
78 [20]. There is limited data on investigating the genetic causes of CH in Bangladesh. However, we
79 have performed several genetic studies and found mutations in patients with thyroid
80 dyshormonogenesis [21] and thyroid dysgenesis [22].

81 High-resolution melting (HRM) curve analysis is one of the molecular tests, which is a high
82 throughput real-time PCR technique based on the melting properties of double-stranded DNA.
83 HRM can differentiate genetic variations such as homozygous or heterozygous states for specific
84 mutations compared to the wild-type state in various genetic diseases, including autosomal
85 recessive, autosomal dominant, and X-linked recessive disorders [23-26].

86 This study aimed to establish HRM curve analysis as a supplementary screening approach of
87 Sanger sequencing targeting three common mutations in Bangladeshi patients. It could play an
88 essential role in screening mass populations since it is faster, cheaper, and more reliable to detect
89 genetic variations for improving the dimensions of newborn screening, which is neglected in
90 Bangladeshi children.

91

92 **2. Methods and Materials**

93 **2.1. Study participant enrolment and specimen collection**

94 We enrolled a total of 36 confirmed cases of congenital hypothyroid children with
95 dysmorphogenesis confirmed by an ultrasonogram of the thyroid gland in the clinical settings of
96 the National Institute of Nuclear Medicine and Allied Sciences (NINMAS) and Department of
97 Endocrinology, Bangabandhu Sheikh Mujib Medical University (BSMMU), Dhaka, Bangladesh.

98

99 **2.2. Ethics approval and consent to participate**

100 This study was approved by the Ethical Review Board for Human Studies of BSMMU and the
101 Human Participants Committee, University of Dhaka (CP-4029) on 16 May 2017. After obtaining
102 the ethical approval, we enrolled patients and collected their specimens from 1 June 2017 to 31
103 December 2019. Blood specimens were collected from the participants with informed written
104 consent from their parents or guardians.

105

106 **2.3. Laboratory investigation**

107 **2.3.1. DNA isolation, PCR amplification, and Sanger Sequencing**

108 Blood specimens (3 mL) were collected, and genomic DNA was isolated using the QIAGEN
109 FlexiGene® DNA Kit, followed by PCR and Sequencing [19]. After that, 20 pre-sequenced
110 specimens were subjected to HRM, and then 16 unknowns were tested.

111

112 **2.3.2. Method setup and validation of High-Resolution Melt curve analysis**

113 For analysis of *TPO* gene mutations by HRM method, we targeted three nonsynonymous
114 mutations in the *TPO* gene identified by Sanger sequencing. For this purpose, we designed three
115 sets of primers for detecting c.1117G>T and c.1193G>C mutations in exon eight and c.2173A>C
116 mutation in exon 12. The primer sequences are listed in Table 1. First of all, those mentioned
117 above, 20 pre-sequenced specimens with known mutations were used as reference samples to set
118 up the HRM method. Homozygous, heterozygous, and wild-type specimens for the specific
119 mutations were subjected to HRM curve analysis. Finally, 16 unknown samples were run to
120 validate the method. These 16 samples were further tested by Sanger sequencing to confirm the
121 mutation and validate the HRM approach.

122 **Table 1: List of primers used in HRM curve analysis**

Primer name	Mutation (nucleotide position)	Primer sequences (5'-3')	Product size (base pair)
TPO_G1117T_Ex8	c.1117G>T	Forward: CGCCTACCTGCCCTTCGTGC	101
		Reverse: CGTCTCCGGCCAGGAAGCAG	
TPO_G1193C_Ex8	c.1193G>C	Forward: CTGCTTCCTGGCCGGAGACG	65
		Reverse: ACAGCGTGTGCAGTGCCGTCAG	
TPO_A2173C_Ex12	c.2173A>C	Forward: AGACTTTGAGTCTTGTGACAGC	90
		Reverse: GTGAGAGGAGACCGAACTTCACC	

123
124 To amplify the target sequence, a master mix was prepared following the protocol provided with
125 the Precision Melt Supermix kit (Bio-Rad). To a reaction mixture of 5 μ L of 2X precision melt
126 super mix, 0.2 μ L of each forward and reverse primer and 1 μ L of DNA (50 ng); 3.6 μ L nuclease-
127 free water were added to make the reaction volume up to 10 μ L. Moreover, for detection of
128 c.1193G>C mutation by HRM, 8mM MgCl₂ was added to the reaction mixture, and the reaction
129 volume was adjusted accordingly. The cyclic condition was divided into two steps, namely real-
130 time PCR amplification followed by melt curve analysis using a single program. The real-time
131 PCR-based HRM was performed on a CFX96 Touch™ Real-Time PCR machine (Bio-Rad). The
132 real-time PCR cyclic condition was as follows: initial denaturation at 95°C for 3 min; 40 cycles of
133 denaturation at 95°C for 10 s, annealing at 60°C for 15 s and extension at 72°C for 15 s. After

134 completion of the real-time PCR, the subsequent melt curve program was initiated through cycles
135 of denaturation at 95°C for 30 s, renaturation at 60°C for 1 min, and then melting at 65°C to 95°C
136 with an increment of 0.1°C per 5 s for c.1117G>T and c.2173A>C mutations. And notably, an
137 increment of 0.2°C per 5 s was used for c.1193G>C mutation. After completion of the real-time
138 PCR-HRM, the data were analyzed using Precision Melt Analysis™ Software (BioRad). The melt
139 curve shape sensitivity for cluster detection was set to 100%. The difference in the T_m threshold
140 for the cluster detection was set to 0.1 to 0.2, and the normalized and temperature-shifted views
141 were used for analysis. The results of pre-sequenced samples were compared with HRM analysis,
142 and an additional 16 unknown samples were subjected to validate the HRM method using the same
143 procedure that was followed for the pre-sequenced known samples. Finally, the normalized melt
144 curve and the difference curves for both wild-type and mutant specimens (homozygous and
145 heterozygous) were calculated and analyzed to detect the mutations in the *TPO* gene.

146

147 **3. Results**

148 Among 36 participants, 21 (58.33%) were males, and 15 (41.67%) were females. The average age
149 of the participants was 7.97±4.29 (years) mean± SD, and the BMI was 17.0±4.4 (Kg/m²) mean±
150 SD.

151 **3.1. Screening of c.1117G>T mutation using HRM analysis**

152 To establish a rapid HRM-based screening approach targeting the c.1117G>T variant, a pair of
153 primers (TPO_G1117T_Ex8) was designed that flanked the c.1117G>T variant. Then, the pre-
154 genotyped samples were subjected to real-time PCR followed by HRM analysis. The fluorescence
155 started to drop quickly at the initial melting phase for heterozygous samples. However, in the later
156 phase of melting, the homozygous samples started to lose fluorescence intensity quicker than the
157 heterozygous samples, and as a consequence, they crossed each other at a certain point of melting,
158 making them distinguishable from each other. Similar to the normalized melting curve (Fig 1), the
159 temperature-shifted difference curve could generate distinctive melting patterns for the wild-type,
160 homozygous and heterozygous specimens (Fig 2). The reliability of the method was further
161 validated by analyzing 16 unknown samples with dyshormonogenesis. At first, these samples were
162 tested by HRM, and then Sanger sequencing was done to check the sensitivity and specificity of
163 the method. A total of 5 specimens had c.1117G>T variant in heterozygous states, six specimens

164 were in a homozygous state, and the remaining 5 had the wild type allele. The HRM result was
165 consistent with the sequencing data, implying that sensitivity and specificity for detecting the
166 c.1117G>T variant was 100% for both homozygous and heterozygous alleles.

167 **Fig 1.** Normalized melt curves for the specimens targeting the c.1117G>T variant in exon-8.

168 Normalized melt curves showing that the specimens with homozygous and heterozygous states are clearly
169 distinguishable from the wild-type specimens, as manifested by the difference in relative fluorescence unit.

170

171 **Fig 2.** Difference curves generated by specimens targeting the c.1117G>T variant in exon-8. Discernable changes in
172 three difference curves were showing that the specimens with homozygous and heterozygous states are clearly
173 distinguishable from the wild type allele, as manifested by the difference in relative fluorescence unit.

174

175 **3.2. Screening of c.1193G>C mutation using HRM analysis**

176 The second set of primers, namely TPO_G1193C_Ex8, was used for the analysis of the c.1193G>C
177 variant by the HRM approach. When the pre-genotyped samples were subjected to HRM analysis,
178 three different clusters were observed in the melt curve analysis. One of the clusters corresponded
179 to the heterozygous samples; the other two were for the homozygous samples and for the wild-
180 type samples (Fig 3). However, in the difference curve analysis, three different clusters were
181 clearly observed for homozygous, heterozygous, and wild-type variants of c.1193G>C (Fig 4). A
182 similar observation was observed with 16 unknown samples that were subjected to HRM analysis.
183 Four out of 16 samples came out as heterozygous by HRM analysis, and this result was consistent
184 with the sequencing data. However, eight homozygous and four wild-type samples formed
185 different clusters in this case. This observation implies that both heterozygous and homozygous
186 states for c.1193G>C variant could be detected with 100% sensitivity and specificity.

187 **Fig 3.** Normalized melt curves generated by specimens targeting the c.1193G>C variant in exon-8. Discernable
188 changes in normalized melt curves were showing that the specimens with homozygous (orange color) and
189 heterozygous (green color) states are clearly distinguishable from the wild type (purple color) alleles, as manifested
190 by the difference in relative fluorescence unit.

191 **Fig 4.** Difference curves for specimens targeting the c.1193G>C variant in exon-8. Discernable changes in difference
192 curves were showing that the specimens with homozygous and heterozygous states are clearly distinguishable from
193 the wild-type states, as manifested by the difference in relative fluorescence unit.

194

195 **3.3. Screening of c.2173A>C mutation using HRM analysis**

196 The third set of primers, namely TPO_A2173C_Ex12, was used to analyze another TPO gene
197 mutation designated as c.2173A>C. The pre-genotyped wild type, homozygous c.2173A>C, and
198 heterozygous c.2173A>C specimens were subjected to HRM analysis. The wild type, homozygous
199 and heterozygous variants formed distinct clusters (Fig 5 and Fig 6). The homozygous c.2173A>C
200 substitution resulted in an increase in melting temperature, and thus, the specimens with
201 homozygous c.2173A>C variant had higher fluorescence intensity than that with the wild-type
202 allele during melting, as manifested by the relative fluorescence unit (Fig 5). On the other hand,
203 although the specimens with the heterozygous c.2173A>C variant followed a melting pattern with
204 lower fluorescence intensity initially compared to the wild type, and the melting curve patterns
205 almost overlapped with each other in a later stage (upper panel of Fig 5). Thus, homozygous
206 c.2173A>C, heterozygous c.2173A>C, and the wild-type alleles were discernable from each other.
207 Similar to the normalized melting curve, the difference curve analysis could also distinguish
208 different states involving the c.2173A>C variant (Fig 6). HRM analysis of 16 unknown samples
209 targeting the c.2173A>C variant was also 100% sensitive and specific. The HRM approach showed
210 that 5 out of 16 unknown samples were wild type, 6 were homozygous, and the rest 5 were
211 heterozygous. Sequencing of those 16 unknown samples revealed that the PCR HRM-based result
212 was consistent with the sequencing result.

213 **Fig 5.** Normalized melt curves for specimens targeting the c.2173A>C variant in exon-12. Discernable changes in
214 normalized melt curves were showing that the specimens with homozygous and heterozygous states are clearly
215 distinguishable from the wild-type alleles, as manifested by the difference in relative fluorescence unit.

216 **Fig 6.** Differential curves for specimens targeting the c.2173A>C variant in exon-12. Discernable changes in
217 difference curves showing specimens with homozygous and heterozygous states are clearly distinguishable from the
218 wild type, as manifested by the difference in relative fluorescence unit.

219

220 **4. Discussion**

221 Congenital hypothyroidism (CH) is the most common cause of intellectual disabilities in children
222 [27]. If early detection of CH is performed and treatment is initiated within 28 days of birth, clinical
223 complications can be reversed by treatment with Levothyroxine, which is very easy to administer

224 and affordable. Although 11 genes have been reported to be responsible for all CH cases with
225 genetic aetiology, only seven genes are responsible for thyroid dyshormonogenesis, and published
226 data have suggested that one of the major genes for thyroid dyshormonogenesis is thyroid
227 peroxidase (TPO), and its mutations are inherited in an autosomal recessive manner to cause the
228 disease [13, 28, 29]. TPO enzyme catalyzes the iodine oxidation process in the thyroid hormone
229 synthesis pathway [30]. To date, approximately 60 mutations in the *TPO* gene have been reported
230 in a total of 17 exons in the *TPO* gene [14, 31-33]. Global publications on the *TPO* gene in
231 hypothyroid patients demonstrated that most of the mutations were confined between exon 7 and
232 exon 14, and very few mutations had been identified outside this region [32][34]. Although the
233 mutations had been detected as homozygous or heterozygous states, our study confirmed that both
234 alleles of the *TPO* gene of all 36 hypothyroid patients had been affected by mutations, further
235 confirming the recessive pattern of this disease. The identified nonsynonymous mutations had
236 previously been reported to be pathogenic or disease-causing mutations [12, 18].

237 A genetic study investigated that mutation c.1117G>T and c.2173A>C showed a non-enzymatic
238 reaction rate, and mutation c.1193G>C showed a slightly reduced enzymatic reaction rate
239 compared to the wild-type TPO protein [34]. Our previous study identified four common mutations
240 in the hotspot region from exon 8 to exon 12 in the TPO gene and studied their effect on the 3D
241 structure of the TPO protein [19]. Since we found these common mutations in Bangladeshi
242 patients, we aimed to establish an alternative method of Sanger sequencing to screen the patients.
243 In Bangladesh, there is very little information about newborn screening and the genetic aetiology
244 of CH. High-resolution melting (HRM) methodology represents a significant advancement in
245 mutation detection over the years. The HRM method has been established for the detection of
246 variants of the beta-globin gene in thalassemia patients and G6PD deficiency in Bangladesh [24,
247 35].

248 The genetic study is important to investigate the cause of CH. There are some screening methods
249 for the diagnosis of CH, such as measurement of serum/blood TSH, T3, and T4. However, these
250 approaches can only confirm the CH cases but not the actual aetiology. That is, the conventional
251 screening method for CH cannot say whether it is acquired or genetic. If the actual aetiology is
252 known, the duration of treatment can be defined based on the causes. If it is due to a genetic cause,
253 the patients could be enrolled for levothyroxine treatment for their whole life. On the other hand,
254 treatment should be continued for the first three years of life for an acquired cause [20]. So, the

255 treatment strategy will be different for CH cases with genetic aetiology and other reasons for CH
256 with dys hormonogenesis. If the genetic basis of CH is defined in the country, carrier screening is
257 possible to target the underlying genetic cause. If the parents are found to be carriers of CH
258 involving the TPO gene, their children or newborns could be screened, and appropriate measures
259 can be taken, such as early initiation of treatment, which would help to prevent mental retardation.
260 Late diagnosis of CH is common in our country, and an initial pilot study suggested that late-
261 diagnosed hypothyroid children had clinical complications even under levothyroxine treatment in
262 Bangladesh. So newborn screening should be a common practice for early CH diagnosis to prevent
263 mental retardation due to late diagnosis.

264 The present study aimed to establish HRM-targeted mutations c.1117G>T, c.1193G>C, and
265 c.2173A>C commonly found in Bangladeshi patients. To validate the method, we designed
266 primers covering the mutational hotspot, keeping the product size between 65-101 base pairs,
267 which fulfilled the requirement of the HRM strategy [36]. To establish HRM, the samples with
268 heterozygous, homozygous, and wild-type alleles were subjected to an experiment. For the first
269 set of primers targeted the mutation c.1117G>T, both homozygous and heterozygous states were
270 clearly distinguishable from wild-type alleles. However, c.1193G>C mutation was much more
271 difficult to differentiate due to the formation of a similar number of hydrogen bonds for G>C
272 substitution, and thus similar level bond energy was involved for both the wild type and mutant
273 variants. To overcome these difficulties, the optimum concentration of MgCl₂ was determined to
274 be 8 mM for detection of a single G>C point mutation by HRM because 8 mM MgCl₂
275 concentration could clearly distinguish among homozygous, heterozygous, and wild-type alleles.
276 This showed that MgCl₂ could have an effect on HRM studies to differentiate different states of
277 mutation of G/C alleles. For the c.1193G>C mutation, the melt curve showed almost similar
278 patterns among the samples with the wild-type allele and also samples with homozygous and
279 heterozygous alleles. However, the temperature-shifted curve could clearly differentiate all the
280 states. Different studies demonstrated that the HRM method could not distinguish purine to
281 pyrimidine nucleotide substitution, such as A to T or G to C substitution, due to the same melting
282 temperature [36-38]. For the third mutation, c.2173A>C, Adenine nucleotide was substituted by
283 Cytosine nucleotide, and due to the difference in bond energy between Purine and pyrimidine
284 group, the melting temperature was shifted for both heterozygous and homozygous states
285 compared to the wild type state. The temperature-shifted pattern was differentiated in such a

286 manner that the wild type had a lower T_m pattern compared to the heterozygous and homozygous
287 states.

288 Although Sanger sequencing is the gold standard for mutation detection, HRM can be used as a
289 fast and less expensive supplemental approach with 100% sensitivity and specificity for screening
290 and detection of mutations in the TPO gene in Bangladeshi patients. Since TPO gene mutation is
291 inherited in an autosomal recessive manner to cause dysmorphogenesis, this HRM method can
292 also investigate its carrier state.

293

294 **5. Conclusion**

295 High-resolution melt curve analysis could be an alternative approach for screening common
296 mutations in the *TPO* gene in Bangladeshi patients with thyroid dysmorphogenesis so that
297 complications of late-diagnosed patients can be prevented by early screening and initiation of
298 treatment in a different strategy.

299

300 **Acknowledgements**

301 The authors are thankful to University Grants Commission (UGC) of Bangladesh for its
302 generous support.

303

304 **References**

- 305 1. Rastogi MV, LaFranchi SH. Congenital hypothyroidism. *Orphanet journal of rare diseases*.
306 2010;5(1):17.
- 307 2. Razavi Z, Mohammadi L. Permanent and transient congenital hypothyroidism in Hamadan West
308 Province of Iran. *International journal of endocrinology and metabolism*. 2016;14(4).
- 309 3. Grüters A, Krude H. Detection and treatment of congenital hypothyroidism. *Nature Reviews*
310 *Endocrinology*. 2012;8(2):104.
- 311 4. LaFranchi SH, Austin J. How should we be treating children with congenital hypothyroidism?
312 *Journal of Pediatric Endocrinology and Metabolism*. 2007;20(5):559-78.
- 313 5. Klett M. Epidemiology of congenital hypothyroidism. *Experimental and Clinical Endocrinology &*
314 *Diabetes*. 1997;105(S 04):19-23.
- 315 6. Harris KB, Pass KA. Increase in congenital hypothyroidism in New York State and in the United
316 States. *Molecular genetics and metabolism*. 2007;91(3):268-77.
- 317 7. Deladoëy J, Bélanger N, Van Vliet G. Random variability in congenital hypothyroidism from thyroid
318 dysgenesis over 16 years in Quebec. *The Journal of Clinical Endocrinology & Metabolism*. 2007;92(8):3158-
319 61.

- 320 8. Olney RS, Grosse SD, Vogt RF. Prevalence of congenital hypothyroidism—current trends and
321 future directions: workshop summary. *Pediatrics*. 2010;125(Supplement 2):S31-S6.
- 322 9. Hasan M, Nahar N, Ahmed A, Moslem F. Screening for congenital hypothyroidism—a new era in
323 Bangladesh. *SOUTHEAST ASIAN JOURNAL OF TROPICAL MEDICINE AND PUBLIC HEALTH*. 2004;34:162-4.
- 324 10. Park S, Chatterjee V. Genetics of congenital hypothyroidism. *Journal of medical genetics*.
325 2005;42(5):379-89.
- 326 11. Grasberger H, Refetoff S. Genetic causes of congenital hypothyroidism due to
327 dysmorphogenesis. *Current opinion in pediatrics*. 2011;23(4):421.
- 328 12. Avbelj M, Tahirovic H, Debeljak M, Kusekova M, Toromanovic A, Krzisnik C, et al. High prevalence
329 of thyroid peroxidase gene mutations in patients with thyroid dysmorphogenesis. *European journal of*
330 *endocrinology*. 2007;156(5):511-9.
- 331 13. Rivolta CM, Esperante SA, Gruñeiro-Papendieck L, Chiesa A, Moya CM, Domené S, et al. Five novel
332 inactivating mutations in the thyroid peroxidase gene responsible for congenital goiter and iodide
333 organification defect. *Human mutation*. 2003;22(3):259-.
- 334 14. Bakker B, Bikker H, Vulmsa T, de Randamie JS, Wiedijk BM, de Vijlder JJ. Two decades of screening
335 for congenital hypothyroidism in The Netherlands: TPO gene mutations in total iodide organification
336 defects (an update). *The Journal of Clinical Endocrinology & Metabolism*. 2000;85(10):3708-12.
- 337 15. Kotani T, Umeki K, Kawano Ji, Suganuma T, Hishinuma A, Ieiri T, et al. Partial iodide organification
338 defect caused by a novel mutation of the thyroid peroxidase gene in three siblings. *Clinical endocrinology*.
339 2003;59(2):198-206.
- 340 16. Rodrigues C, Jorge P, Soares JP, Santos I, Salomao R, Madeira M, et al. Mutation screening of the
341 thyroid peroxidase gene in a cohort of 55 Portuguese patients with congenital hypothyroidism. *European*
342 *Journal of Endocrinology*. 2005;152(2):193-8.
- 343 17. Wu J, Shu S, Yang C, Lee C, Tsai F. Mutation analysis of thyroid peroxidase gene in Chinese patients
344 with total iodide organification defect: identification of five novel mutations. *Journal of Endocrinology*.
345 2002;172(3):627-35.
- 346 18. Balmiki N, Bankura B, Guria S, Das TK, Pattanayak AK, Sinha A, et al. Genetic analysis of thyroid
347 peroxidase (TPO) gene in patients whose hypothyroidism was found in adulthood in West Bengal, India.
348 *Endocrine journal*. 2014;61(3):289-96.
- 349 19. Begum M, Islam MT, Hossain SR, Bhuyan GS, Halim MA, Shahriar I, et al. Mutation spectrum in
350 TPO gene of Bangladeshi patients with thyroid dysmorphogenesis and analysis of the effects of different
351 mutations on the structural features and functions of TPO protein through in silico approach. 2019;2019.
- 352 20. Büyükgebiz A. Newborn screening for congenital hypothyroidism. *Journal of Pediatric*
353 *Endocrinology and Metabolism*. 2006;19(11):1291-8.
- 354 21. Begum MN, Mahtarin R, Ahmed S, Shahriar I, Hossain SR, Mia MW, et al. Investigation of the
355 impact of nonsynonymous mutations on thyroid peroxidase dimer. 2023;18(9):e0291386.
- 356 22. Begum MN, Mahtarin R, Islam MT, Ahmed S, Konika TK, Mannoor K, et al. Molecular investigation
357 of TSHR gene in Bangladeshi congenital hypothyroid patients. 2023;18(8):e0282553.
- 358 23. Yan J-b, Xu H-p, Xiong C, Ren Z-r, Tian G-l, Zeng F, et al. Rapid and reliable detection of glucose-6-
359 phosphate dehydrogenase (G6PD) gene mutations in Han Chinese using high-resolution melting analysis.
360 *The Journal of Molecular Diagnostics*. 2010;12(3):305-11.
- 361 24. Islam MT, Sarkar SK, Sultana N, Begum MN, Bhuyan GS, Talukder S, et al. High resolution melting
362 curve analysis targeting the HBB gene mutational hot-spot offers a reliable screening approach for all
363 common as well as most of the rare beta-globin gene mutations in Bangladesh. *BMC genetics*.
364 2018;19(1):1.
- 365 25. Bono C, Nuzzo D, Albeggiani G, Zizzo C, Francofonte D, Iemolo F, et al. Genetic screening of Fabry
366 patients with EcoTILLING and HRM technology. *BMC research notes*. 2011;4(1):323.

- 367 26. Bataille S, Berland Y, Fontes M, Burtsey S. High Resolution Melt analysis for mutation screening in
368 PKD1 and PKD2. *BMC nephrology*. 2011;12(1):57.
- 369 27. Grosse SD, Van Vliet G. Prevention of intellectual disability through screening for congenital
370 hypothyroidism: how much and at what level? *Archives of disease in childhood*. 2011:archdischild190280.
- 371 28. Pannain S, Weiss RE, Jackson CE, Dian D, Beck JC, Sheffield VC, et al. Two different mutations in
372 the thyroid peroxidase gene of a large inbred Amish kindred: power and limits of homozygosity mapping.
373 *The Journal of Clinical Endocrinology & Metabolism*. 1999;84(3):1061-71.
- 374 29. Fugazzola L, Mannavola D, Vigone MC, Cirello V, Weber G, Beck-Peccoz P, et al. Total iodide
375 organification defect: clinical and molecular characterization of an Italian family. *Thyroid*.
376 2005;15(9):1085-8.
- 377 30. Taurog A, Dorris M, Doerge DR. Evidence for a radical mechanism in peroxidase-catalyzed
378 coupling. I. Steady-state experiments with various peroxidases. *Archives of biochemistry and biophysics*.
379 1994;315(1):82-9.
- 380 31. Belforte FS, Miras MB, Olcese MC, Sobrero G, Testa G, Muñoz L, et al. Congenital goitrous
381 hypothyroidism: mutation analysis in the thyroid peroxidase gene. *Clinical endocrinology*. 2012;76(4):568-
382 76.
- 383 32. Bikker H, Vulsma T, Baas F, de Vijlder JJ. Identification of five novel inactivating mutations in the
384 human thyroid peroxidase gene by denaturing gradient gel electrophoresis. *Human Mutation*.
385 1995;6(1):9-16.
- 386 33. Kimura S, Hong YS, Kotani T, Ohtaki S, Kikkawa F. Structure of the human thyroid peroxidase gene:
387 comparison and relationship to the human myeloperoxidase gene. *Biochemistry*. 1989;28(10):4481-9.
- 388 34. Guria S, Bankura B, Balmiki N, Pattanayak AK, Das TK, Sinha A, et al. Functional analysis of thyroid
389 peroxidase gene mutations detected in patients with thyroid dysmorphogenesis. *International journal*
390 *of endocrinology*. 2014;2014.
- 391 35. Islam MT, Sarker SK, Talukder S, Bhuyan GS, Rahat A, Islam NN, et al. High resolution melting curve
392 analysis enables rapid and reliable detection of G6PD variants in heterozygous females. *BMC genetics*.
393 2018;19(1):58.
- 394 36. Stomka M, Sobalska-Kwapis M, Wachulec M, Bartosz G, Strapagiel D. High Resolution Melting
395 (HRM) for High-Throughput Genotyping—Limitations and Caveats in Practical Case Studies. *International*
396 *journal of molecular sciences*. 2017;18(11):2316.

397

398 **Supporting information**

399 **S1 Table. Sequenced samples that were used for the HRM method setup.**

400 **S2 Table. Unknown samples used for HRM method validation.**

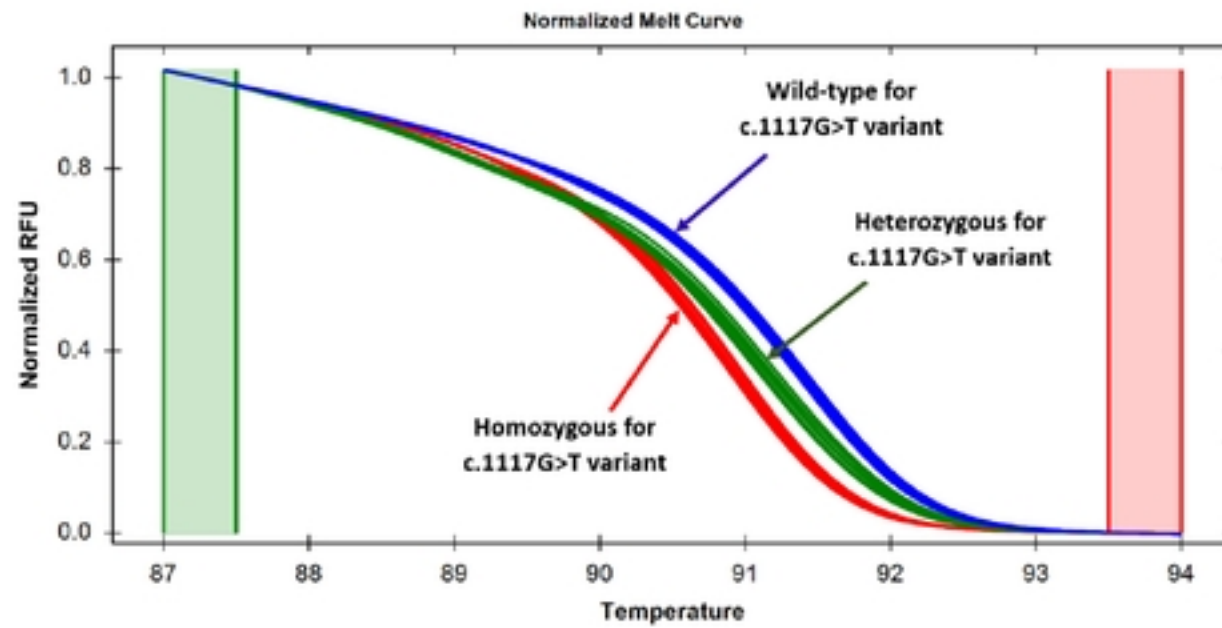


Fig 1. Normalized melt curves for the specimens targeting the c.1117G>T variant in exon-8. medRxiv preprint doi: <https://doi.org/10.1101/2023.10.17.23297147>; this version posted October 18, 2023. The copyright holder for this preprint (which was not certified by peer review) is the author/funder, who has granted medRxiv a license to display the preprint in perpetuity. It is made available under a [CC-BY 4.0 International license](https://creativecommons.org/licenses/by/4.0/).

Normalized melt curves showing that the specimens with homozygous and heterozygous states are clearly distinguishable from the wild-type specimens, as manifested by the difference in relative fluorescence unit.

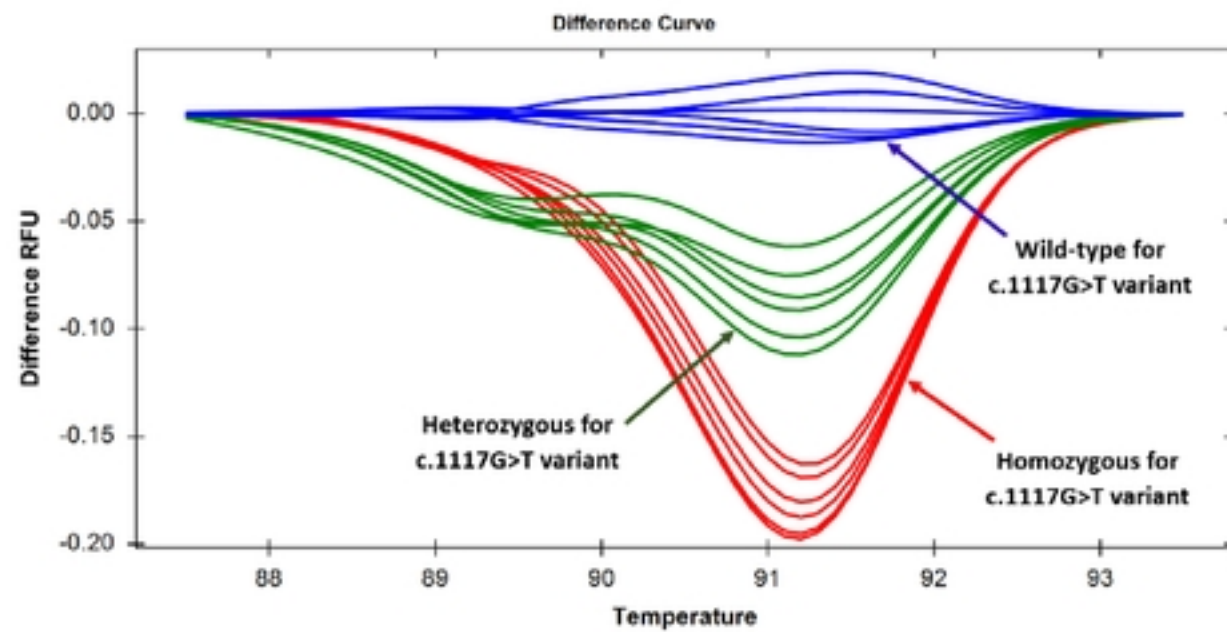


Fig 2. Difference curves generated by specimens targeting the c.1117G>T variant in exon-8. Discernable changes in three difference curves were showing that the specimens with homozygous and heterozygous states are clearly distinguishable from the wild type allele, as manifested by the difference in relative fluorescence unit.

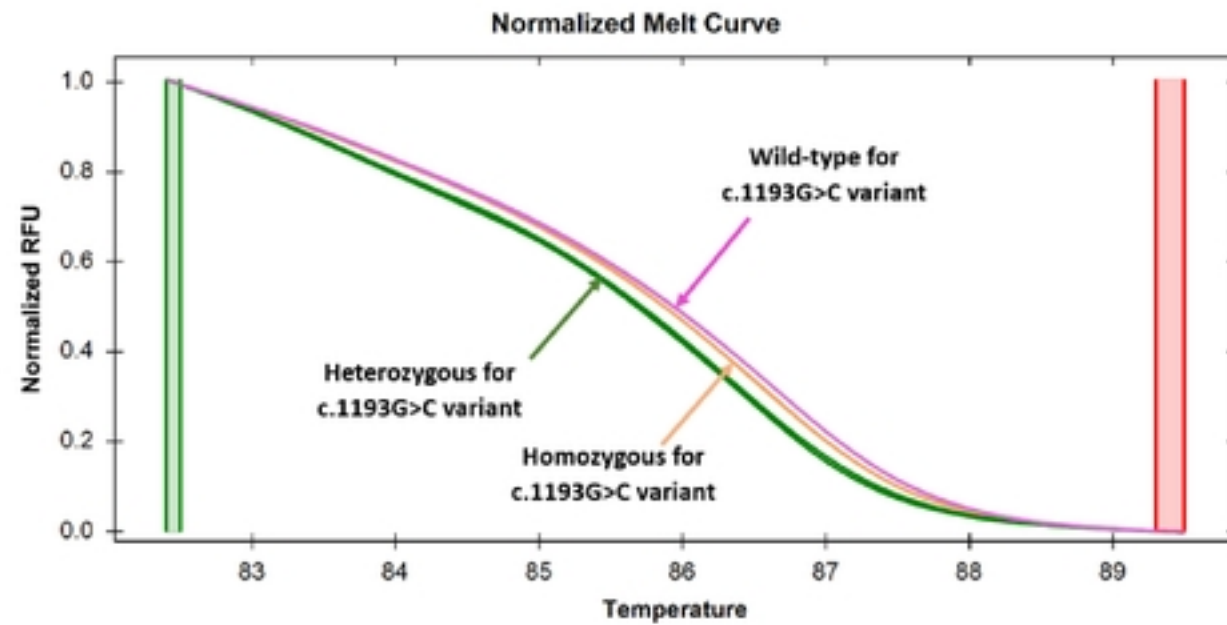


Fig 3. Normalized melt curves generated by specimens targeting the c.1193G>C variant in exon-8. Discernable changes in normalized melt curves were showing that the specimens with homozygous (orange color) and heterozygous (green color) states are clearly distinguishable from the wild type (purple color) alleles, as manifested by the difference in relative fluorescence unit.

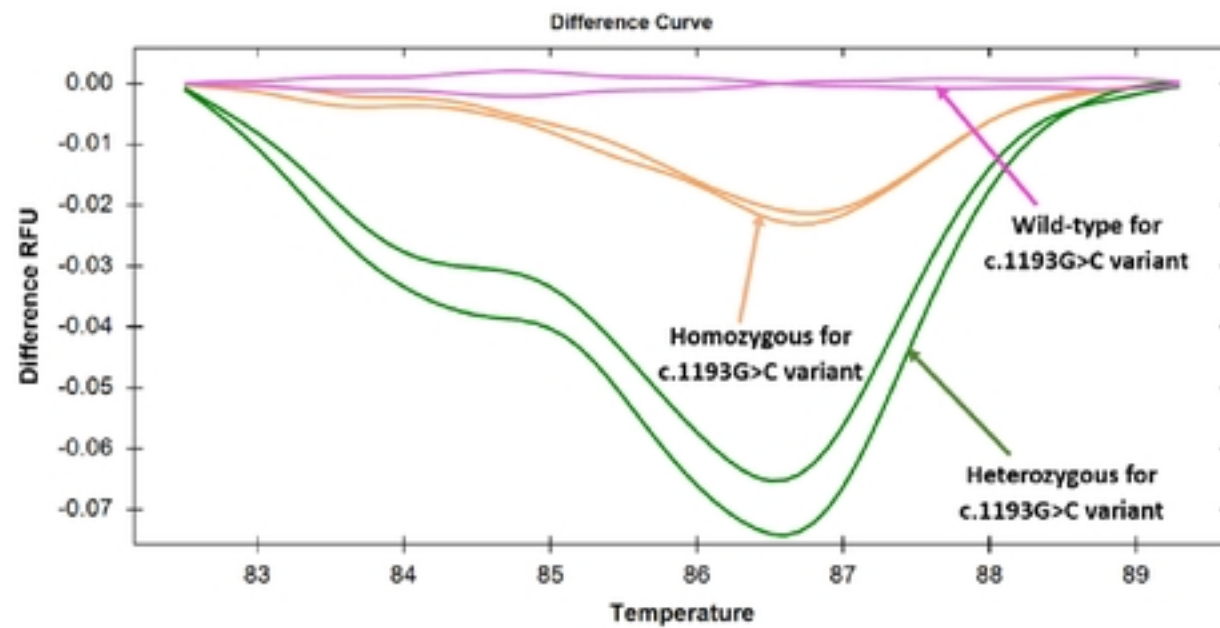
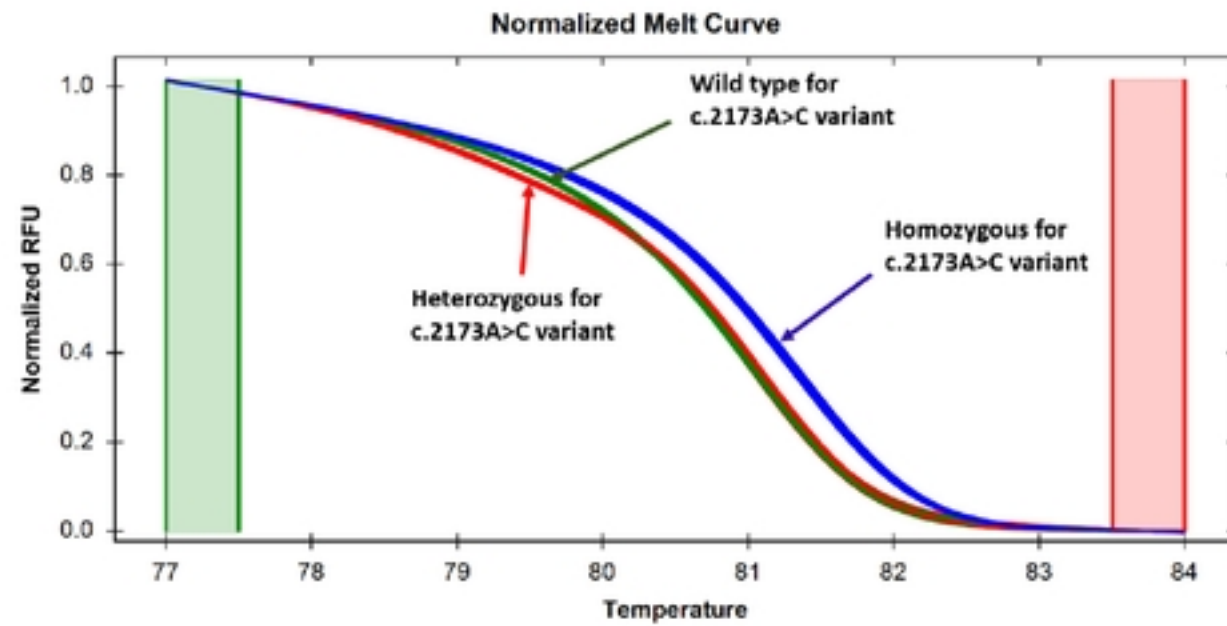


Fig 4. Difference curves for specimens targeting the c.1193G>C variant in exon-8. Discernable changes in difference curves were showing that the specimens with homozygous and heterozygous states are clearly distinguishable from the wild-type states, as manifested by the difference in relative fluorescence unit.



medRxiv preprint doi: <https://doi.org/10.1101/2023.10.17.23291147>; this version posted October 16, 2023. The copyright holder for this preprint (which was not certified by peer review) is the author/funder, who has granted medRxiv a license to display the preprint in perpetuity. It is made available under a [CC-BY 4.0 International license](https://creativecommons.org/licenses/by/4.0/).

Discernable changes in normalized melt curves were showing that the specimens with homozygous and heterozygous states are clearly distinguishable from the wild-type alleles, as manifested by the difference in relative fluorescence unit.

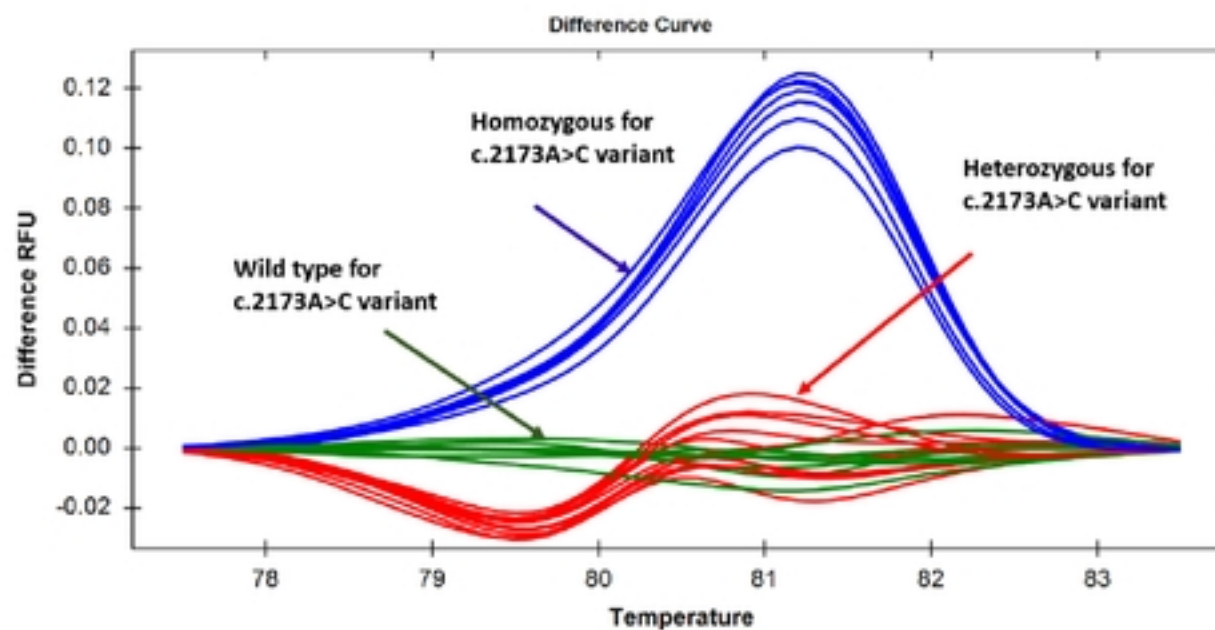


Fig 6. Differential curves for specimens targeting the c.2173A>C variant in exon-12. Discernable changes in difference curves showing specimens with homozygous and heterozygous states are clearly distinguishable from the wild type, as manifested by the difference in relative fluorescence unit.